Journal of Constructional Steel Research 101 (2014) 143–157

Contents lists available at ScienceDirect

Journal of Constructional Steel Research

Progressive collapse potential of a typical steel building due to blast attacks

H.M. Elsanadedy *,[1], T.H. Almusallam, Y.R. Alharbi, Y.A. Al-Salloum, H. Abbas

MMB Chair for Research and Studies in Strengthening and Rehabilitation of Structures, Department of Civil Engineering, King Saud University, P.O. Box 800, Riyadh 11421, Saudi Arabia

ARTICLE INFO

Article history:
Received 10 February 2014
Accepted 17 May 2014
Available online 11 June 2014

Keywords:
Progressive collapse
Steel building
Blast load
LS-DYNA
FE analysis

ABSTRACT

The recent terrorist attacks all around the world and the evidence of the threats found especially in the Kingdom of Saudi Arabia have prompted the concerned authorities to address the risks to the critical infrastructure of the Kingdom. Understanding of the progressive collapse mechanism is an essential step to protect buildings against blast attacks. Buildings are very vulnerable to progressive collapse if one or more columns are lost due to extreme loadings. It is also important to study the likelihood of progressive collapse of buildings in Riyadh to avoid catastrophic events. The paper presents progressive collapse analysis of a typical multi-storey steel framed building in Riyadh to establish its vulnerability when subjected to accidental or terrorist attack blast scenarios. A commercial finite element (FE) package (LS-DYNA) was used to simulate the building response under blast generated waves. The numerical modeling was validated using the results of a published example of tubular steel beam subjected to blast load. Based on the FE analysis results, recommendations are given to mitigate (or control) the progressive collapse potential of steel buildings.

1. Introduction

Progressive collapse refers to the phenomenon in which the local damage of a primary structural element leads to total or partial structural system failure, without any proportionality between the initial and final damage. Even if the probability of structural collapse is low, if it occurs, it can cause significant losses. In the past few decades, many incidents of the total or partial collapse of structures due to fire, explosions or impacts have occurred.

The progressive collapse phenomena was first brought to engineers' attention due to the collapse of a 22-storey building in Ronan Point, London (UK), as a result of a gas explosion in 1968 [1,2]. The research in this area accelerated due to two significant terrorist attacks in the United States that resulted in the structural collapse of the buildings: the Alfred P. Murrah Federal Building collapse in Oklahoma City (USA) bombing in 1995 [3] and the destruction of the World Trade Center (WTC), in New York (USA) in 2001 [4–7].

Most of the published progressive collapse analyses of entire buildings or their components are based on the alternate load path method with column removal. The DoD criteria [8] and the GSA 2003 Guidelines [9] regarding load configurations and quantification of collapse are usually adopted. However, differences are encountered in the numerical technique applied to predict structural behavior.

In Marjanishvili and Agnew [10], an explanation of four methods used to perform progressive collapse analysis (LS: Linear Static; NLS: Nonlinear Static; LD: Linear Dynamic; and NLD: Nonlinear Dynamic) in SAP2000 is presented. Fu [11] performed nonlinear dynamic analyses of a 20-storey 3D structure and found that the columns that are adjacent to the removed column should be designed with an axial force twice that of the static axial force obtained when applying the DL + 0.25LL (DL: Dead load and LL: Live load) load combination. Furthermore, Fu [11] found that column removal in the top stories leads to higher vertical deformations because fewer stories participate in the absorption of the released energy. Mohamed [12] analyzed 3D concrete structures and investigated the shear stresses that resulted from the torsion in the beam connected to the corner column being removed. The shear stresses in these scenarios lead to brittle failure of the beam, but the 2D analysis models could not trace them.

Khandelwal et al. [13] analyzed the progressive collapse potential of seismically designed steel-braced frames, using explicit transient dynamic simulations. The study used the alternate path method on previously designed 10-storey prototype buildings. The structural response was predicted using calibrated 2D macro-models built as a combination of beam-column and discrete spring finite elements.

Ruth et al. [14] analyzed 2D and 3D steel frames and illustrated that using a load factor of 2 may be conservative, whereas using a load factor of approximately 1.5 captures better dynamic effects when static analyses are performed. However, they stated that using a load factor of 2 may be more appropriate for structures of high ductility provided the behavior of the materials was not elastic-perfectly plastic and the materials harden after yielding. As a result, their research suggested

* Corresponding author. Tel.: +966 597938718.
E-mail address: elsanadedy@yahoo.com (H.M. Elsanadedy).
[1] On leave from Dept. of Civil Engineering, Helwan University, Cairo, Egypt.

http://dx.doi.org/10.1016/j.jcsr.2014.05.005
0143-974X/

that a load factor of 2 should be used for important structures and 1.5 for other structures.

Powel [15] compared LS, NLS, and NLD analyses and found that if a load factor of 2 is used in static analyses, it can display very conservative results. Tsai and Lin [16] evaluated the progressive collapse resistance of reinforced concrete (RC) buildings and demonstrated that nonlinear static analyses provide more conservative estimate for the collapse resistance than nonlinear dynamic analyses. They also found that the load factor decreases with the increase in the displacement of the removed column point. Sucuoglu et al. [17] found that the 2D frames that contained a removed column sustained most of the load that was created due to the column removal. Therefore, to evaluate the vertical displacement, the plastic hinge distribution, and rotation in 3D frames, it is sufficient to analyze the 2D frames that contain the removed column.

Kim and Kim [18] studied the progressive collapse of the steel moment resisting frames. It was observed that the linear static analyses provide lower structural responses than nonlinear dynamic analyses and the results varied more significantly depending on the variables such as applied load, location of column removal, or number of building storey. However, the linear static analysis procedure provides a more conservative decision for the progressive collapse potential of model structures.

Kim and Dawoon [19] investigated the effect of the catenary action on the progressive collapse potential of steel moment frame structures. According to the nonlinear static push-down analysis results, the contribution of the catenary action to the progressive collapse demonstrated that the potential of the structures increases as the number of stories and bays increase. Grierson et al. [20] presented a method for conducting a linear static progressive collapse analysis. They modeled the reduced stiffness during the progressive collapse using an equivalent spring method.

Izzuddin et al. [21,22] presented a simplified method for nonlinear static analysis of steel structures. In their research, simplifications were applied to the method. Lee et al. [23] also developed a simplified trilinear model for the relationship between the vertical resistance and chord rotation of the double span beam. This model depends explicitly on the beam length (l) and beam section depth (d). A response was obtained for three values of l/d: 10, 15, and 20. Lee et al. [23] state that for other values of l/d, linear interpolation should be used.

Naji and Irani [24] presented a simplified analysis procedure for the progressive collapse analysis of steel structures using the load displacement and capacity curve of a fixed end steel beam. The results of the proposed method were in good agreement with nonlinear dynamic analysis results. Finally, an explicit expression for the dynamic increase factor (DIF) was established for elastic-perfectly plastic and elastic plastic with catenary action behavior.

Almusallam et al. [25] carried out progressive collapse analysis of a commercial RC building located in the city of Riyadh and subjected to different blast scenarios. A 3-D FE model of the structure was created using a ready-made commercial package. Blast loads were treated as dynamic pressure-time history curves applied to the exterior elements. It was depicted that the shortcomings of notional member removal requirements of many codes might be addressed by improved blast analysis through the use of solid elements with the provision of element erosion. Thus, the regulatory requirements of approximate static structural response for the failure of vertical members under blast load got replaced in the analysis by the improved dynamic phenomenon of the collapse of members. Effects of erosion and cratering were studied for different scenarios of the blast. It was found that the effect of cratering has quite an impact on the behavior of a structure subjected to a close-in detonation as evident from the two scenarios; with and without cratering.

A search of literature has revealed numerous numerical studies on the vulnerability of existing steel buildings to progressive collapse. However, only a limited number of studies are available on the assessment of progressive collapse potential of existing steel buildings when subjected to blast threat scenarios. Major drawback of the code provisions for the assessment of progressive collapse potential of buildings is the absence of appropriate criteria for deciding the column removal which is primarily related to the threat scenarios for the building. In fact, a validated numerical analysis procedure that is simple, yet accurate, and investigates the effect of different blast threat scenarios on the vulnerability of existing steel buildings to progressive collapse could not be found. The lack of such research creates a challenge for the investigation of numerical modeling using the FE method, despite FE being an efficient and cost-effective numerical tool to model the structural behavior of steel buildings under blast loads.

In this study, a simplified nonlinear dynamic (NLD) analysis procedure was conducted to establish the vulnerability of a typical multistorey steel framed building in Riyadh when subjected to accidental or terrorist attack blast scenarios. A ready-made commercial FE package LS-DYNA [26] was used to simulate blast loads for this purpose. The FE modeling was carried out in two stages – the local model stage to assess the individual columns performance against blast pressures [27] and the global modeling stage to assess the overall response of the structure due to the failure of the critical columns. The numerical modeling was validated using the results of a published example of tubular steel beam subjected to blast load.

2. Building description

A typical six storied (G + 5) commercial steel building taken for the present investigation is located in a congested urban area in the city of Riyadh. The building is adjacent to two other buildings in the North and East directions. The front of the building is located in the South direction and is overlooking a main street of 30 m width. The main street is normally abuzz with hundreds of cars lining the traffic lights and huge numbers of pedestrians walking along the walkway which gives it an impression of being congested although the street is fairly wide. The West side of the building is overlooking a side street of 15 m width. The building is a steel framed structure with the layouts of beams and columns as shown in Fig. 1. The structure has a RC core for lift. The floors consist of one-way joist steel floor system. The peripheral facade consists of in-filled brick masonry with glazed windows. The typical cross section of beams and columns at a typical floor level is shown in Fig. 1. There are a total of fifteen outer and three interior columns. There are no expansion joints in the building.

3. Blast threat scenario identification

The assessment of blast resistance of a building requires defining the level of threat. The possible threats may be numerous but the present study considers the terrorist bombing involving the intentional explosion outside the building. The threat for a conventional bomb is defined by three equally important elements, namely the type of explosive, charge weight and the stand-off distance. There are many explosive devices such as Ammonium-Nitrate Fuel Oil (ANFO) mixture, Trinitrotoluene (TNT), C4 and Semtex, etc. that may be used by terrorists, but so as to standardize the criteria, the charge weight of an explosive device in terms of the equivalent weight of TNT was considered. Thus there are only two parameters to be considered in the blast analysis i.e. the charge weight and the stand-off distance.

The layout of the building is rectangular in plan. The main entrance and exit of the building is located in the South side. The building is located on a major road with the South face of the building facing the road. The front face has street-side parking and sidewalk. The major threat to the building from terrorist bombing is through explosion in a parked vehicle. The layout of the building and its surroundings suggest that a vehicle may be parked close to the building on the South face which is facing the road. Thus the minimum stand-off distance of the location of explosion for the building was taken as 2 m. Two possible critical

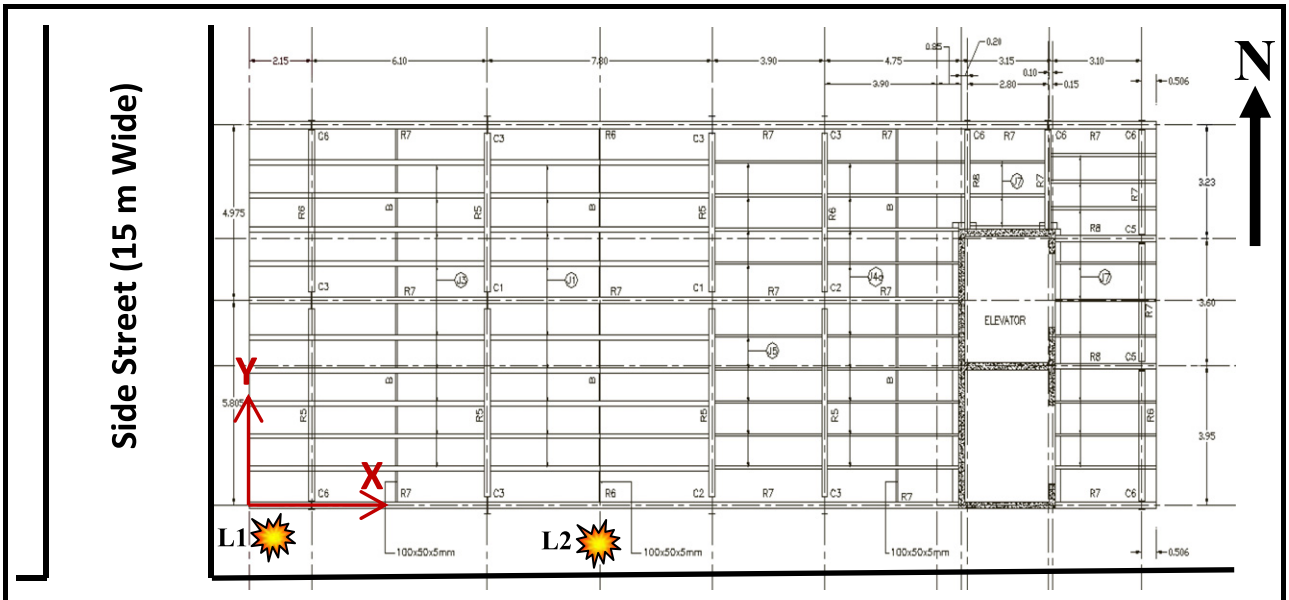

Blast Locations: L1 (0.736, -1.414, 1.5 m) & L2 (12.15, -2.0, 1.5 m)

* Reference level (0.0 m) is the street level.

Main Street (30 m Wide)

Dimensions of beam sections

Main beams					
Mark	Dimension	Size (mm)			
		d	b	t_f	t_w
R5	H450×200×9	450	200	14	9
R6	H400×200×8	400	200	13	8
R7	H346×174×7	346	174	9	7
R8	H298×149×6	298	149	8	5.5
Joists					
J1	H346×174×6	346	174	9	6
J3	H298×149×6	298	149	8	5.5
J4A	H248×124×5	248	124	8	5
J5	H200×100×6	200	100	8	5.5
J7	H175×90×5	175	90	8	5

Dimensions of column sections

Mark	Dimension	Size (mm)			
		d	b	t_f	t_w
C1	H444×300×15	444	300	18	15
C2	H344×348×10	344	348	16	10
C3	H368×356×15	368	356	15	15
C5	H300×300×10	300	300	15	10
C6	H250×250×9	250	250	14	9

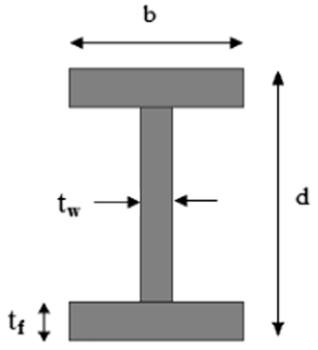

- Storey height = 3.6 m
- Thickness of RC slabs = 120 mm
- Thickness of RC core wall = 200 mm
- Thickness of masonry walls = 200 mm

Fig. 1. Building plan at typical floor level.

locations of explosion, as shown in Fig. 1, were considered in the study. It was assumed that the explosive is carried in a small vehicle due to which the height of explosion was taken 1.5 m above the ground/street level. The charge weight for both explosions was taken as 500 kg of TNT. The coordinates of the locations of explosion sites with respect to the coordinate axes are given in Fig. 1. The selection of these two scenarios depends upon the layout of the building with respect to the street, the stand-off-distance provided, and the available access to the building.

3.1. Mechanism of air blast loading on structures

The blast loads may be generated by nuclear or non-nuclear explosives. The nuclear explosions generate very high pressure waves which are accompanied with excessive heat whereas the non-nuclear explosions generate high pressure waves and the heat generated is only nominal. This paper deals with the non-nuclear explosives which are associated with the acts of terrorism. Different sources of explosives result in different amounts of energy release but most of the explosive materials can be represented in terms of the conventional explosive TNT.

Air explosions result in the rapidly expanding gaseous reaction products which compress the surrounding air and move it outwards with a high velocity leading to the formation of blast waves. The rapid pressure increase at the shock front of blast waves is followed by an exponential decay down to the ambient pressure and a long phase of negative pressure i.e. below ambient, as shown in Fig. 2. The overpressure-time history of a blast wave (Fig. 2) is usually described by Friedlander's equation [28]:

$$p = p_s(1-x)e^{-bx} \tag{1}$$

where,

$$x = \frac{(t-t_a)}{T_s} \tag{2}$$

where p is the static overpressure at time t whose peak value is p_s, T_s is the duration of the positive phase, t_a is the arrival time and b is a positive constant called the waveform parameter that depends on the value of p_s. The value of p_s being quite large as compared to the negative pressure, the negative phase impulse is usually ignored especially for rigid structures like RC frames.

For the estimation of blast wave parameters involved in Eqs. (1) & (2), a large number of models are available in literature. The present study employs ConWep [29] for the estimation of these parameters. ConWep calculates the blast parameters using the equations given by Kingery–Bulmash [30,31], which is based on the data obtained from explosive tests using weights ranging from less than 1 kg to over 400,000 kg.

When the blast waves encounter a rigid barrier, all flow behind the wave is stopped and the pressure increases many folds. The peak reflected pressure p_r can be obtained from Rankine–Hugoniot relationships for an ideal gas, using [32]:

$$p_r = 2p_s\left(\frac{7p_o + 4p_s}{7p_o + p_s}\right) \tag{3}$$

The magnification factor for the peak reflected pressure thus varies from 2 to 8.

The reflected pressure and positive phase duration found from ConWep for 500 kg charge weight considered in the study are plotted in Fig. 3. The results of one higher and one lower charge weights are also plotted in this figure. Due to the limitation of minimum range for the applicability of ConWep, minimum range for this figure is taken as 2 m.

4. Finite element analysis

The progressive collapse analysis of the building was performed using LS-DYNA finite element code – version 971 [26]. Though the blast analysis of building may be carried out by modeling the structure using solid elements for beams, columns, slabs and façade and exposing it to blast which may be applied to the exposed faces of different elements [25] but the time, effort and space requirement will be enormous; this approach may not be adopted by structural designers. Further the interpretation of the results of such a model would be an uphill task and may not be practically feasible for studying the behavior of various structural elements. The development of an efficient procedure of progressive collapse analysis requires that the building should be modeled using beam and shell elements, which are practically feasible not only for modeling but also for the interpretation of results. The employment of beam elements for columns and beams creates problems in the application of blast pressure-time history, which may be applied on the surfaces but the surfaces of these elements are lost in their modeling. When such a model, employing beam and shell elements, is exposed to blast, the loads to columns are only transmitted through façade elements. These elements, being weaker, will transfer small magnitude of blast loads and the significant blast load on those columns due to their direct exposure is not applied. Thus, the simplified modeling employing beam and shell elements requires indirect approach for incorporating these effects which are not accounted for in this analysis. It is due to these reasons that the finite element modeling was carried out in two stages – the local model stage to assess the individual columns performance against blast pressures and the

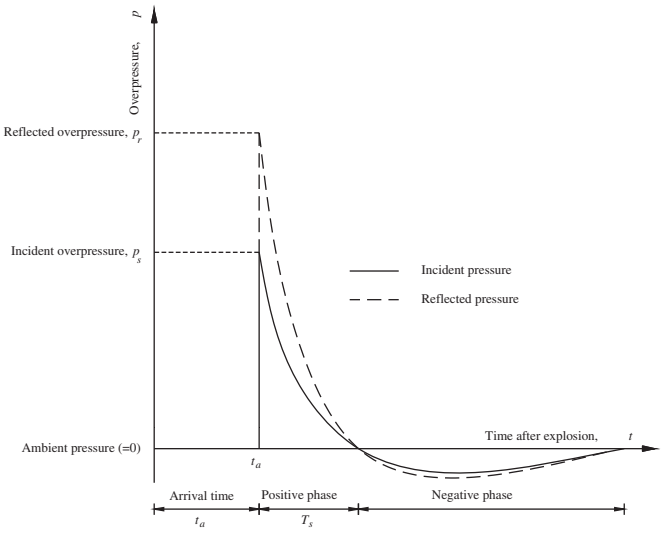

Fig. 2. Air blast pressure-time history.

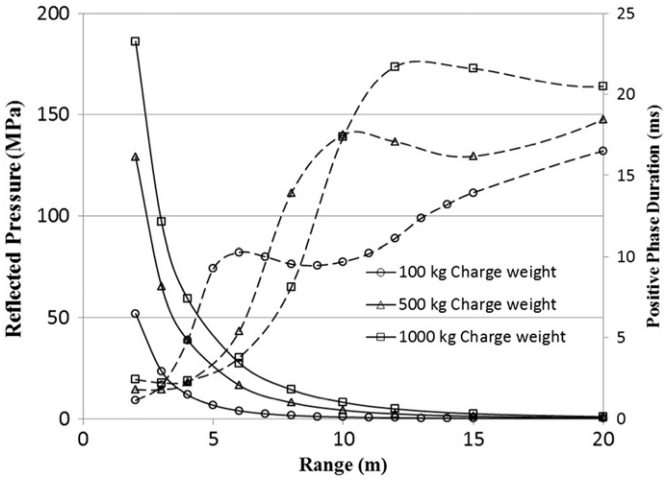

Fig. 3. Reflected pressure and positive phase duration for different charge weights (Note: Solid line is used for reflected pressure and dashed line for positive phase duration).

global modeling stage to assess the overall response of the structure due to the failure of the critical columns. The columns that are expected to be severely damaged were removed from the global model at the arrival time of blast. The level of damage to the columns was decided based on an independent local column analysis. The local analysis was performed by modeling the column using solid elements. The local column analysis was performed for finding out the critical distance within which a column gets severely damaged. This simplified procedure of progressive collapse analysis is based on the following assumptions:

i) The local column analysis assumes direct exposure of column to blast pressure. The assumption is valid for exterior columns but the interior columns will be exposed to blast after the removal of façade and internal walls.
ii) Although the columns beyond the critical distance may also undergo minor damage due to the exposure of blast but this has been ignored. This is done partly to compensate the conservatism in the total column removal approach and partly for the sake of simplification.
iii) The top and bottom ends of column are taken as fixed in the local column analysis. This is done to compensate for the conservatism in the total column removal approach and more importantly for the sake of simplification. The error introduced as a result of this assumption is not significant.
iv) The impact of falling floors and elements on other members is ignored. Thus contact forces due to the strike of a part on another are ignored. The strike of floors and elements on the ground is also ignored.
v) The temperature rise due to the impact of fragments and due to the blast waves is ignored.
vi) As the blast is assumed to occur above ground inside a vehicle, the blast waves transmitted through ground are ignored.

4.1. Local model

4.1.1. Model geometry

The critical structural members are the perimeter columns in the vicinity of vehicle carrying explosive device. The number of columns involved in the progressive collapse analysis was decided based on the local analysis of a representative column for which column C1 was used. The precise analysis would however require the repetition of local analysis for other column sections lying within the range of blast. The column was modeled using hexahedron constant stress solid elements with one point integration rule (LS-DYNA default). The one point integration solid element helps in maintaining the numerical stability of the model during the analysis. Fig. 4 shows cross section details and FE mesh of column C1. The column was discretized into 1550 solid elements and 3276 nodes.

4.1.2. Material modeling

The material model used in the local column analysis is Piecewise Linear Plasticity model (material model type 24). This material is suited to model elasto-plastic materials with an arbitrary stress versus strain curve and an arbitrary strain rate dependency. A summary of constitutive parameters used in the analysis are presented in Table 1. The strain rate effect was incorporated by applying the Cowper–Symonds relation, giving yield stress magnification factor as:

$$y = 1 + \left(\frac{\dot{\varepsilon}}{C}\right)^{1/p} \tag{4}$$

where $\dot{\varepsilon}$ is the strain rate. The model parameters C and p were taken as 250 and 1.6, respectively.

4.1.3. Loading and boundary conditions

Fixed boundary conditions were assigned for the top and bottom nodes of the column. The axial load was applied as pressure load at

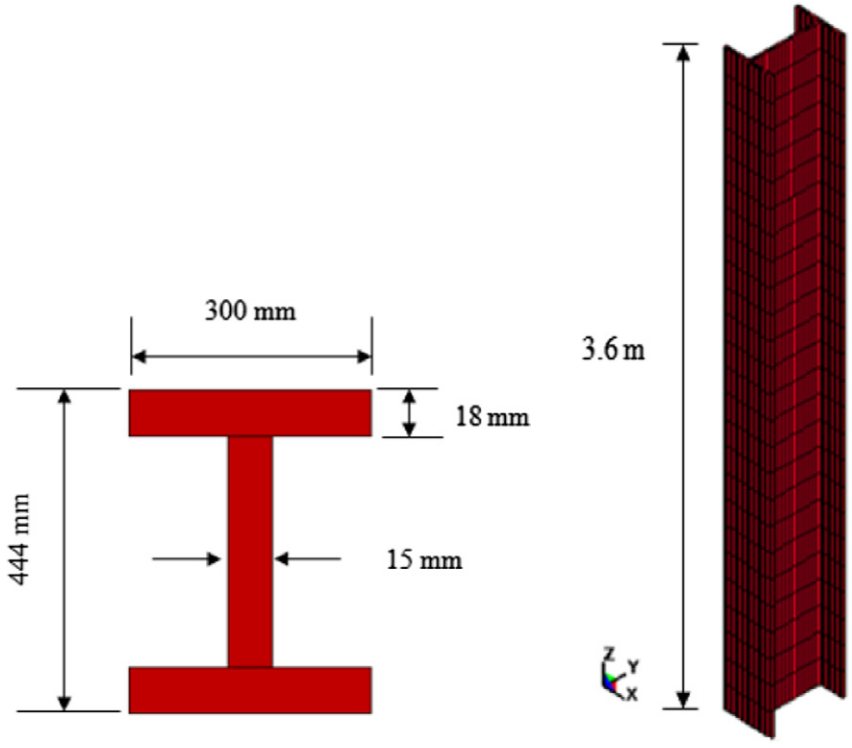

Fig. 4. Mesh discretization of column C1 for local modeling.

Table 1
Constitutive parameters.

Local model								
Material	Constitutive model	Density (kg/m^3)	Young's modulus (MPa)	Poisson's ratio	Yield stress (MPa)	Failure strain		
Steel	Piecewise linear plasticity	7850	200,000	0.3	430	0.1		
Global model – Steel								
Material/structural element	Constitutive model	Density (kg/m^3)	Young's modulus (MPa)	Poisson's ratio	Yield stress (MPa)	Failure strain		
Steel beams/columns	Simplified Johnson/Cook	7850	200,000	0.3	430	0.1		
Global model – Concrete and reinforcement								
Material/structural element	Constitutive model	Density (kg/m^3)	Compressive strength (MPa)	Tensile strength (MPa)	Steel reinforcement			
					Young's modulus (MPa)	Yield stress (MPa)	Percentage, $\rho_x = \rho_y$	Poisson's ratio
RC slab/shear wall	Concrete EC2	2500	30	2.53	200,000	500	0.4%	0.3
Global model – facade								
Material	Constitutive model	Density (kg/m^3)	Young's modulus (MPa)	Poisson's ratio	Yield stress (MPa)	Failure strain		
Masonry facade	Plastic Kinematic	1800	18,000	0.2	15	0.003		

the column top. This axial load was applied as a ramp function over a period of 0.5 s as shown in Fig. 5. A charge of 500 kg equivalent weight of TNT at a variable stand-off distance (8.5–10 m) was considered in the study. The blast loads impinging on the contact segments of the column were calculated using the in-built ConWep function in LS-DYNA [29]. The contact segments of the blast were the solid elements of the front face of the column which were taken to be in contact with the blast. The blast loading was set to trigger at 0.5 s as shown in Fig. 5. The termination time of 2.0 s was set in order to realize the complete blast-related response of the column.

4.2. Global model

4.2.1. Model geometry

The global FE model of the building is shown in Fig. 6. The structure geometry was built based on the available detailed drawings. In the global modeling phase, the elements of the structure were simplified into beam and shell elements. Steel columns and beams were modeled as 2-node axial beam elements with tension, compression, torsion, and bending capabilities. The element has six degrees of freedom at each node: three translations and three rotations about Cartesian axes. The element formulation theory used in the model was Hughes-Liu with cross-section integration. The Hughes-Liu beam is a conventionally integrated element that can model rectangular or circular cross-sections using an array of integration points at the mid-span of the element. RC core walls, RC slabs and masonry façade were modeled using four node quadrilateral and three node triangular shell elements. This element has both bending and membrane capabilities. Both in-plane

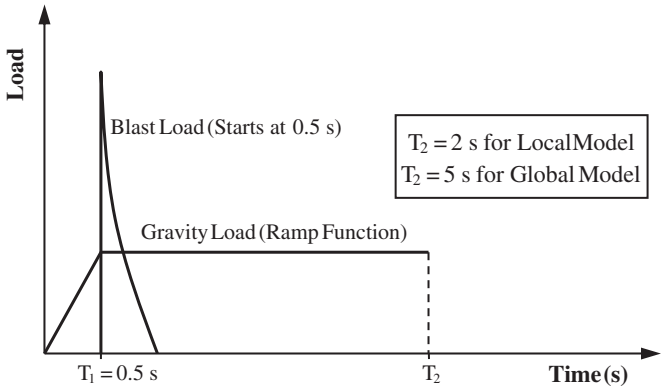

Fig. 5. Loading stages for local and global models.

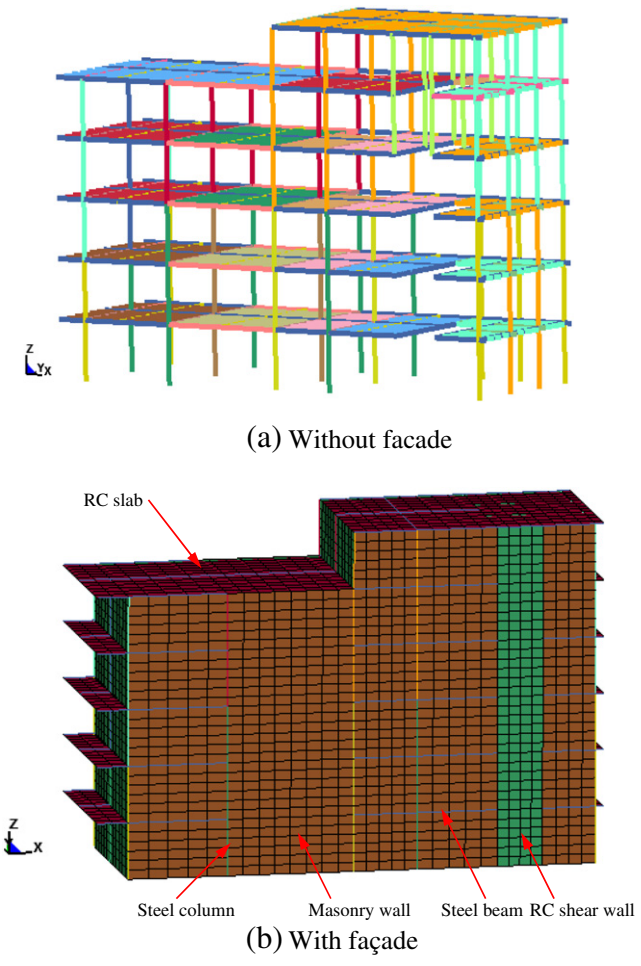

Fig. 6. Finite element model of the building.

and normal loads are permitted. The element has six degrees of freedom at each node: three translations and three rotations about Cartesian axes. Stress stiffening and large deflection capabilities are included. The element formulation theory used in the modeling was Belytschko-Tsay theory [33]. The global FE model has 4246 beam elements representing steel beams and columns in addition to 5852 shell elements representing RC core, RC slabs and masonry facade.

4.2.2. Material modeling

For steel beams and columns, the constitutive model employed was Simplified Johnson/Cook material model (material model type 98), which is suitable for beam elements. In this simplified model, thermal effects are ignored. Failure occurs when the effective plastic strain exceeds the defined effective plastic strain at failure. The strain rate effect is incorporated using Cowper-Symonds formula of Eq. (4). The material model used for the concrete slab and RC core is Concrete Eurocode EC2 (material model type 172), which is suitable for beam and shell elements. The Concrete EC2 material model is capable of representing plain concrete, discrete reinforcement bars, and concrete with smeared reinforcement, which is predominantly used in the global model. The model is capable of representing tensile cracking, compressive crushing, reinforcement yielding, hardening and failure. Cracking in tension occurs when the maximum in-plane stress reaches the tensile strength of concrete. The Plastic Kinematic model (material model type 3) was utilized to model masonry façade. The material properties of the façade components were adopted based on the actual façade system behavior. The failure of the façade system in the model is governed by the failure strain threshold. This modeling approach is adequate as a visual aid to establish the damage on the façade system in a blast event since façade system performance would have a very small contribution towards the overall structural system performance against blast pressures. As the façade is made of concrete masonry blocks, a plastic failure strain of 0.3% was adopted. The constitutive parameters for different elements in the structure are summarized in Table 1. The damping of materials was ignored, which is usually done in blast analysis.

4.2.3. Loading and boundary conditions

Fixed boundary conditions were assigned for the bottom nodes of the ground storey columns. In the analysis, the loads were applied in two stages to account for both gravity and blast loads. The gravity load was applied as a ramp loading function, and maintained constant once it had reached the peak gravity load level at 0.5 s as seen in Fig. 5. The blast pressure was applied to the façade components of the structure using the in-built ConWep function in LS-DYNA [29]. Two potential different scenarios were considered for the blast analysis as shown in Fig. 1. These are: scenario-1 (location L1 in Fig. 1) in which the charge was placed diagonally at the left bottom (South-West) corner of the building, and scenario-2 (location L2 in Fig. 1) in which the charge was placed at the mid-face (South) of the building. For both threat scenarios, the charge was taken as 500 kg equivalent weight of TNT. The blast load applied on the shell elements of outer façade walls gets transmitted to the frames through the common nodes. The blast loading was set to trigger at 0.5 s. At the arrival time of blast, significantly damaged columns identified through local column analysis were deleted through the "restart" option of the program which requires the recalculation of stiffness matrix. The analysis termination time of 5.0 s was set in order to realize the complete blast-related response of the whole building.

4.3. Solution strategy

LS-DYNA uses explicit time integration algorithm for solving the problems, which are less sensitive to machine precision than other finite element solution methods. The benefits of this are greatly improved utilization of memory and disk. An explicit FE analysis solves the incremental procedure and updates the stiffness matrix at the end of each increment of load (or displacement) based on changes in the geometry and the material.

5. Numerical model verification

In order to validate the employed numerical models, a fixed beam of 600 mm span and square hollow steel section of $35 \times 35 \times 1.6$ mm nominal size, tested under a uniform transverse blast load by Jama et al. [34], was modeled by LS-DYNA and a comparison was made between the experimental and numerical results. The beam was tested on a ballistic pendulum in a blast chamber that was used to measure the impulse. The beam was modeled using 4-noded shell elements as shown in Fig. 7. The size of each element was 5×5 mm thus giving 3360 elements and 3388 nodes. Piecewise Linear Plasticity model (material model type 24) was employed for modeling steel and the yield stress of steel was taken as 430 MPa. The top flange of beam was analyzed for five different values of rectangular impulses: 39.1, 49.2, 56.0, 58.3 and 66.8 Ns acting independently. The impulse was converted to pressure using the following formula:

$$P = \frac{I}{A\tau} \tag{5}$$

where I is the impulse, A the area of the top flange of the beam and τ the duration of the blast, which is the time taken for the blast wave to travel from the centre of the beam where detonation was initiated to the supports (approximately taken as 40 μs.). The arrival time of impulse was taken as 0.15 ms. The strain rate effect was incorporated by employing the Cowper-Symonds relation given earlier in Eq. (4), with the model parameters, C and p taken as 250 and 1.6, respectively for yield stress of steel. A comparison of the non-dimensional local deformation of beam obtained from the FE analysis and the experimental results for the five impulses is given in Table 2. It is observed from the table that the predicted values are close to the experimental results with the error ranging from 0.6% to 16.4%. It is also clear that the predicted values follow the same trend of increase in local deformation with increasing magnitude of impulse. Both predicted and observed deflected shapes of the beam for 56.0 Ns impulse and at 0.3 ms are shown in Fig. 8, which indicates good match between the test and FE analysis.

6. Discussion of finite element results

6.1. Local model analysis

The following principles are considered when defining the damage criterion: (1) it should be suitable for the evaluation of the steel column damage from all possible damage modes; (2) it should be related to the

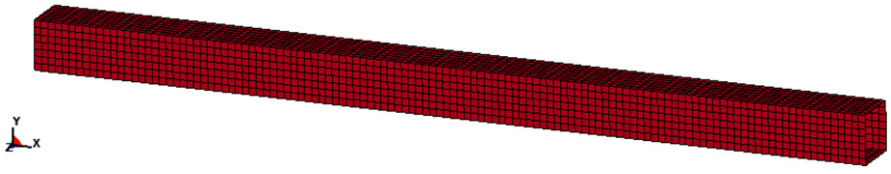

Fig. 7. Finite element model of the beam tested by Jama et al. [30].

Table 2
Comparison of non-dimensional local deformation of beam tested by Jama et al. [34].

Impulse (Ns)	Pressure (MPa)	Non-dimensional local deformation Δ/H^*		
		Experimental	FE	Error (%)
39.1	46.6	0.90	0.80	11.1
49.2	58.6	1.10	0.92	16.4
56.0	66.7	1.00	0.99	0.6
58.3	69.4	1.10	1.03	6.4
66.8	79.5	1.20	1.14	4.8

* H is the depth of beam (=35 mm)

column global properties, besides the column material damage; and (3) it should be easy to use in assessing the column condition and (4) it should be easily obtainable numerically or experimentally. None of the commonly used damage criteria, such as the permanent deflection at the middle of the column, material modulus reduction, the maximum stress or the maximum strain, satisfy the above principles. Considering that the columns are primarily designed to carry the axial loads (horizontal loads are mainly transferred to the rigid floor and the shear wall), the axial load-carrying capacity degradation of steel column was used to quantify column damage. The axial load-carrying capacity degradation is suitable for evaluating the damage to steel columns, as well as the local damage. It is also a parameter that is directly related to the global properties and functionality of the steel column, and can be easily obtained from the numerical simulation or experiments [35]. The damage index D was taken as [35]:

$$D = 1 - \frac{P_{N\_residual}}{P_{N\_design}} \tag{6}$$

where $P_{N\_residual}$ is the residual axial load carrying capacity of the damaged steel column, which can be obtained from the numerical simulation; P_{N_design} is the design axial load-carrying capacity of the undamaged steel column, and it was calculated as per ANSI/AISC 360-05 [36]. In accordance with Shi et al. [35], the degrees of damage are defined as: D = 0–0.2 for low damage level; D = 0.2–0.5 for medium damage level; D = 0.5–0.8 for high damage level; and D = 0.8–1 for collapse.

As mentioned previously, the local column analysis was carried out for stand-off distance varying from 8.5–10.0 m. The progress of deformation of column C1 for 9 m stand-off distance is shown in Fig. 9. The damage index for each stand-off distance is presented in Table 3 and its variation is shown in Fig. 10. It is observed from the figure that column located within a distance of 9 m gets damaged. The number of columns to be deleted in the global analysis was decided based on the results of this analysis. Thus all columns located within a distance of 9 m from the location of blast were deleted in the global analysis.

Although the consideration of fixed end condition of column is an assumption in the local column analysis for the reasons stated in Section 4, however the effect of column end conditions on the local column analysis was studied for hinged top end which is the extreme case of free rotation. The base of the column being connected to the RC raft was taken as fixed. A comparison of the results of analysis for the two end conditions of the column when it is located at 9 m stand-off distance is given in Table 4. Although there is moderate increase in the instantaneous and permanent peak lateral displacements (13.1% and 19.4% respectively) but the increase in the damage index, D, is minimal (2.5%). Moreover, the actual end conditions of the column being in-between the fixed and hinged conditions, the assumption of fixed-fixed column end condition is thus justified for the ground storey columns.

6.2. Global model analysis

6.2.1. Threat scenario 1

The local model analysis results, presented earlier, indicated that three ground storey columns shown enclosed in the shaded area in Fig. 11 will be severely damaged and eventually lose their load carrying capacity and were thus deleted in the global analysis. Initially the model contains all structural elements but at the arrival time of blast (0.5 s) the columns lying within the critical distance were deleted using the "restart" option of LS-DYNA program.

Fig. 12 shows the damage of the façade and the partial collapse of the structure at the end of blast. Due to the loss of the columns in the vicinity of the blast event, the gravity load got transferred to adjacent vertical members such as the next columns and the core structure via flexural action of the floor slab. The partial collapse occurred because the aforementioned flexural stresses exceeded the flexural capacity of the floor slab. Hence, the floor slab was extensively damaged and subsequently lost its load transfer capacity due to the loss of column support. The damage started with the failure of façade and then beams and slabs and subsequently the critical columns which are next to the deleted columns. The failure of façade was due to its direct exposure to blast pressure whereas the failure of beams was due to the loss of column support due to the deletion of columns.

Four critical columns (C6, C3, C1 and C2) located next to the deleted columns, as shown in Fig. 11, were identified for studying their progress of collapse. The response of these columns was studied in terms of the development of axial force in comparison to their ultimate load carrying capacity. The variation of axial force transfer to the critical columns is shown in Fig. 13a–d. The axial force plotted in these figures is for the bottom-most beam element of each column. The negative value of axial force indicates compressive load. Fig. 13a to d depict that the axial force in column increases with the application of gravity loads and it gets stabilized just before the arrival time of blast at 0.5 s. Upon blast arrival, a large redistribution of forces was observed to take place and the column axial force increased significantly before settling down at a steady value after duration of 2.0 s.

The axial load carrying capacity, axial load at service level due to gravity, peak axial force developed in the column due to blast and the steady value of axial force after blast are given in Table 5 for critical columns of blast scenario-1. The axial force developed in columns C6, C3 and C1 were close to the ultimate load carrying capacity causing these columns to fail which was also observed from the run of the program. The axial force developed in column C2 was low and it maintained the load even after the blast; therefore, failure of critical column C2 was not observed in the analysis.

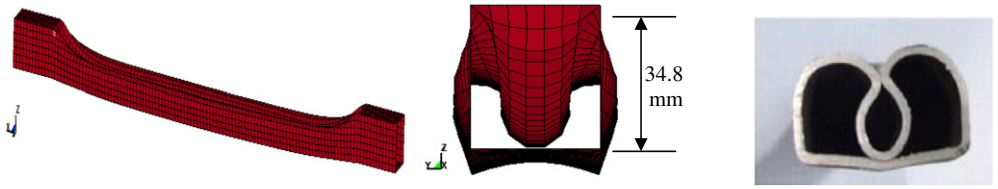

(a) FE analysis (b) Experimental (Jama et al. [34])

Fig. 8. Mid-span deflected shape of beam tested by Jama et al. [30] for 56 Ns impulse at 0.3 ms.

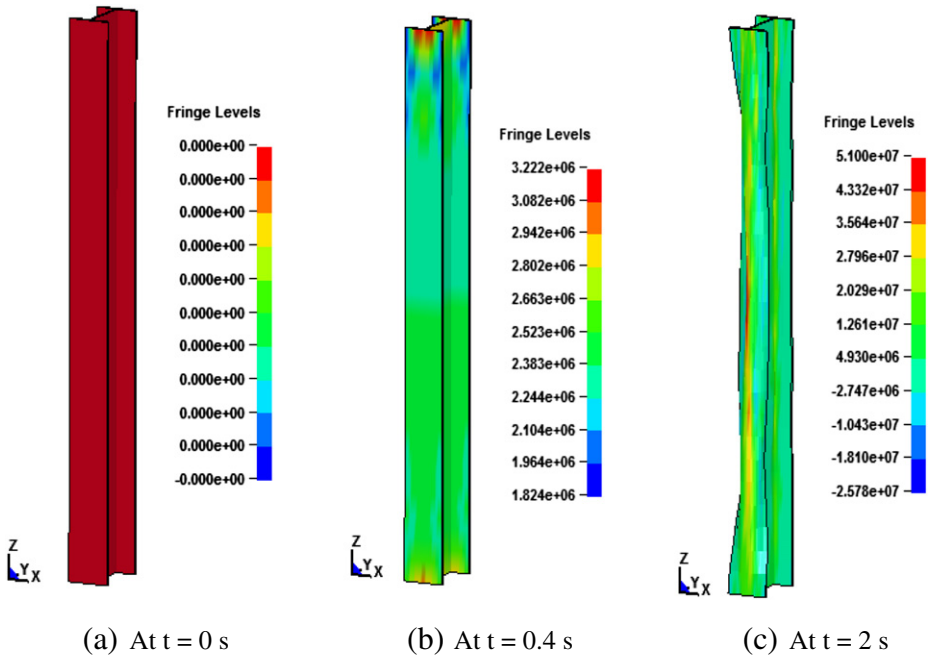

Fig. 9. Damage of column C1 in the local model FE analysis for 9-m stand-off distance showing Von-Mises stress contours.

6.2.2. Threat scenario 2

The local model analysis results indicated that five columns shown enclosed in the shaded area in Fig. 14 will get severely damaged and eventually lose their load bearing capacity and were thus deleted in the global analysis. Initially the model contained all structural elements but at the arrival time of blast (0.5 s) the columns lying within the critical distance were removed using the "restart" option of LS-DYNA program.

Depicted in Fig. 15 are the façade damage and the partial collapse of the building at the end of blast. Due to the loss of the columns in the vicinity of the blast event, the gravity load got transferred to adjacent vertical elements via flexural action of the floor slab. As observed in threat scenario-1, the partial collapse took place because the flexural stresses due to column removal exceeded the flexural capacity of the floor slab and as a result, the slab was extensively damaged and subsequently lost its load transfer capacity. The damage commenced with the failure of façade and then beams and slabs and subsequently the critical columns that are next to the removed ones.

Five critical columns (C6, C3, C3, C3 and C2) located next to the removed columns, as shown in Fig. 14, were identified for studying their progress of collapse. The variation of axial force transfer to the critical columns is shown in Fig. 16a–e. The axial load carrying capacity, axial load at service level due to gravity, peak axial force developed in the column due to blast and the steady value of axial force after blast are presented in Table 6 for the five critical columns of blast scenario-2. The axial force developed in column of location 1 (C6) was close to the ultimate load carrying capacity; this column has failed as observed from the analysis. The axial forces developed in the other four critical columns were lower than their ultimate capacity and they sustained the load even after the blast and as a result, failure of these columns was not identified in the FE analysis.

Table 3
Damage index for column C1.

Stand-off distance (m)	P_{N_design} (kN)	$P_{N\_residual}$ (kN)	Damage index (D)
8.5	6840	1320	0.81
9	6840	1368	0.80
9.5	6840	1573	0.77
10	6840	1792	0.74

7. Comparison with GSA 2003 Guidelines

The GSA 2003 Guidelines [9] were followed to assess the progressive collapse potential of the studied steel building using the simplified linear static (LS) analysis procedure. The results were then compared with the two-stage nonlinear dynamic (NLD) analysis procedure proposed earlier. The building was modeled using the commercial FE package ETABS Nonlinear Version 9.7.4 [37]. Two-node frame elements were used to model steel beams and columns; whereas, four-node shell elements were employed to model RC slabs and RC core walls. The non-structural façade elements were not included in the model. The 3D FE model of the building is shown in Fig. 17. Following the provisions of the GSA 2003 Guidelines, the potential for progressive collapse is assessed using the linear static step-by-step analysis procedure in

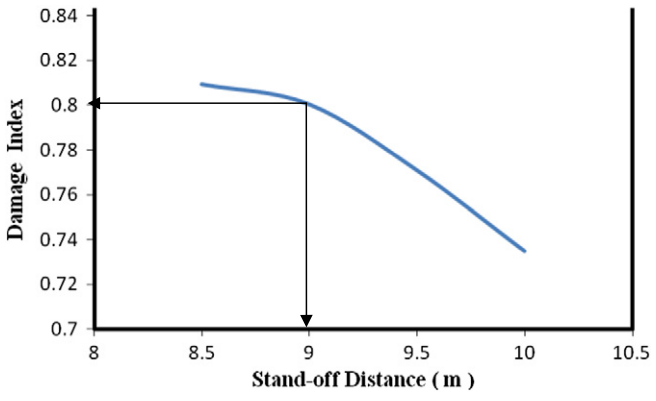

Fig. 10. Damage index for column C1 vs. stand-off distance for 500-kg charge weight.

Table 4
Effect of end conditions on performance of blast-damaged column C1 at 9-m stand-off distance.

Support conditions	Instantaneous peak lateral displacement (mm)	Permanent peak lateral displacement (mm)	Maximum principal stress (MPa)	P_{N_design} (kN)	$P_{N\_residual}$ (kN)	Damage index (*D*)
Fixed-fixed	230.7	86.5	582	6840	1368	0.80
Fixed-pinned*	260.9 (13.1%)	103.3 (19.4%)	586 (0.7%)	6448	1147	0.82 (2.5%)

* Value within brackets is the percentage increase with respect to the fixed-fixed support condition.

three damage analysis cases ("missing column" scenarios), as illustrated in Fig. 18: (i) the loss of a corner column (Scenario S1), (ii) the loss of an exterior column located near the middle of the long side of the building (Scenario S2) and (iii) the loss of an exterior column located near the middle of the short side (Scenario S3). It should be noted that the three scenarios S1 to S3 apply only to ground storey columns. As per

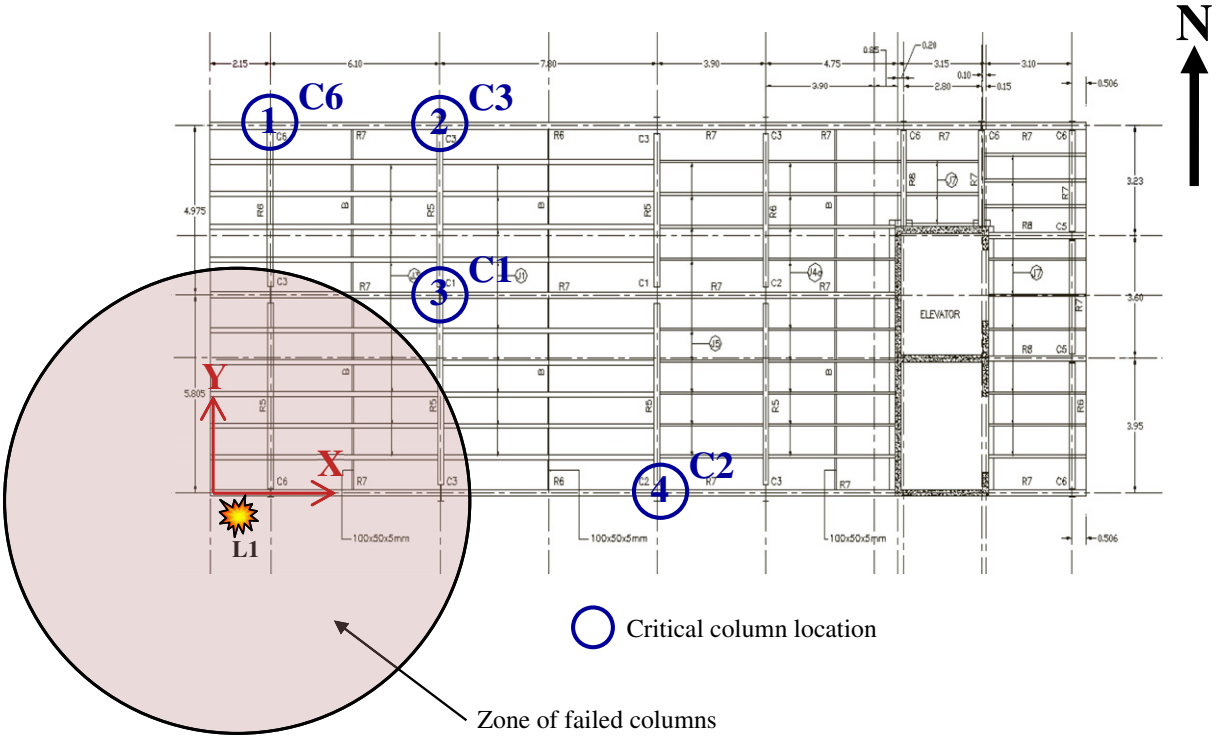

Fig. 11. Zone of failed and critical ground storey columns for blast scenario-1.

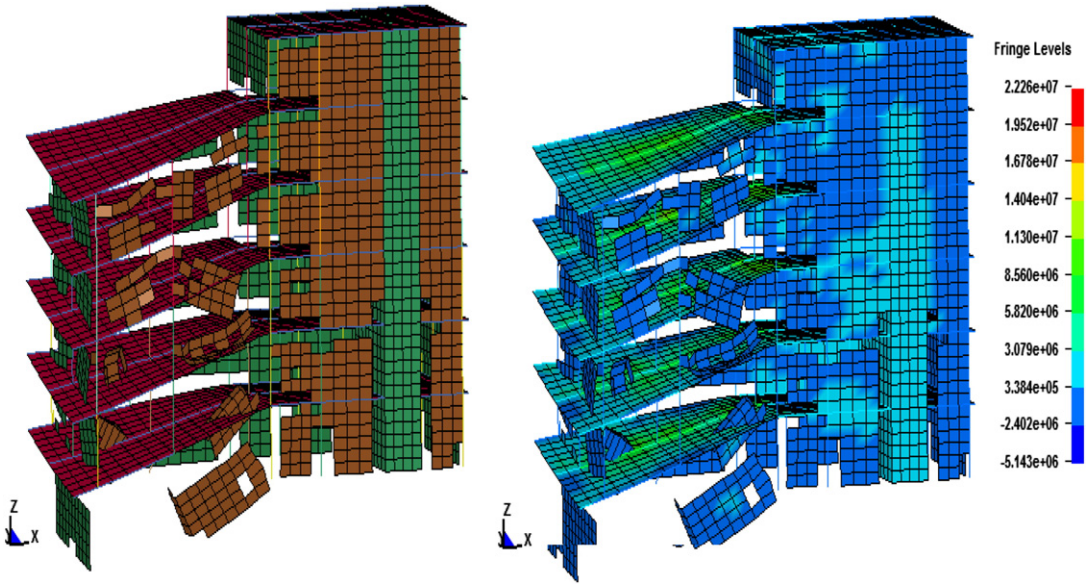

Fig. 12. Partial collapse of building for blast scenario-1.

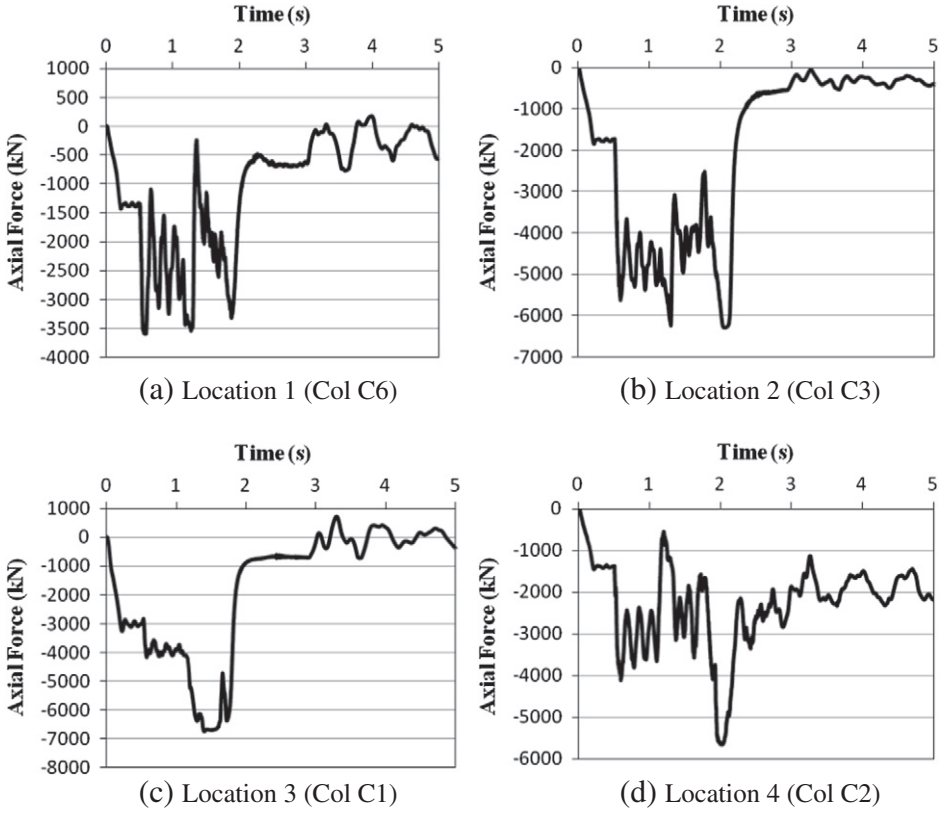

Fig. 13. Variation of axial force with time for critical columns under blast scenario-1.

the GSA 2003 Guidelines, the 3D ETABS model was analyzed under the following gravity load:

$$\text{Load} = 2(\text{DL} + 0.25\text{LL}) \tag{7}$$

where DL is the dead load (self-weight plus a supplementary dead load of 4.0 kN/m^2) and LL is the live load (3.0 kN/m^2). In the GSA Guidelines, live load is reduced to 25% of the full design live load, admitting that the entire LL value is less probable. At the same time, by multiplying the load combination by a factor of two, the GSA 2003 Guidelines [9] take into account – in a simplified approach – the dynamic effect that occurs when a vertical support is instantaneously removed from the structure. After the static analysis, a demand-capacity ratio (*DCR*) is computed for each of the structural members in the building from

$$DCR = \frac{Q_{UD}}{Q_{CE}} \tag{8}$$

where Q_{UD} is the acting force (demand) determined in component (moment, axial force, and shear etc.); and Q_{CE} is the expected ultimate, unfactored capacity of the component (moment, axial force, shear etc.). In the GSA 2003 Guidelines, while computing Q_{CE}, the strength reduction factor is not applied and the nominal material strength may be increased by a strength-increase factor to account for expected actual strength of materials. For steel members, this factor may vary from 1.05 to 1.10, depending on types and age of steel. In this study, a strength increase factor of 1.05 was used for steel beams and columns. As per the GSA 2003 Guidelines, structural elements that have *DCR* values that exceed the allowable value of 2.0 (for typical structural configuration) are considered to be severely damaged or collapsed.

For each missing-column scenario mentioned above, the *DCR* values were calculated automatically by ETABS for all structural members of the building. Table 7 enlists *DCR* values for steel beams due to flexure and shear demands and for steel columns due to axial force-flexure interaction. It is demonstrated from Table 7 that the GSA acceptance criteria ($DCR \leq 2.0$) are fulfilled for the three different column removal scenarios and no further iterations were required. According to the GSA 2003 Guidelines, none of the structural members failed. For scenarios S1 and S3, the *DCR* values exceed 1.0 for 6 and 8 columns (at different stories), respectively, which, as per Marchis et al. [38], indicate a low potential of progressive collapse. For column removal scenario S2, *DCR* values for all columns were less than 1.0, which may point to a no potential of progressive collapse. In conclusion, according to the GSA 2003 Guidelines, the steel building may have a low potential

Table 5
Variation of axial load for critical columns of blast scenario-1.

Column location	Column designation	Axial load capacity (P_N) (kN)	Service load (P_s)		Peak load after blast (P_p)		Steady value after blast (P_t)	
			(kN)	P_s/P_N (%)	(kN)	P_p/P_N (%)	(kN)	P_t/P_N (%)
1	C6	3598	1332	37	3594	99.8	500	14
2	C3	6500	1729	26.6	6305	97	500	8
3	C1	6840	3120	45	6761	98.8	0	0
4	C2	5905	1394	24	5502	93.1	2000	34

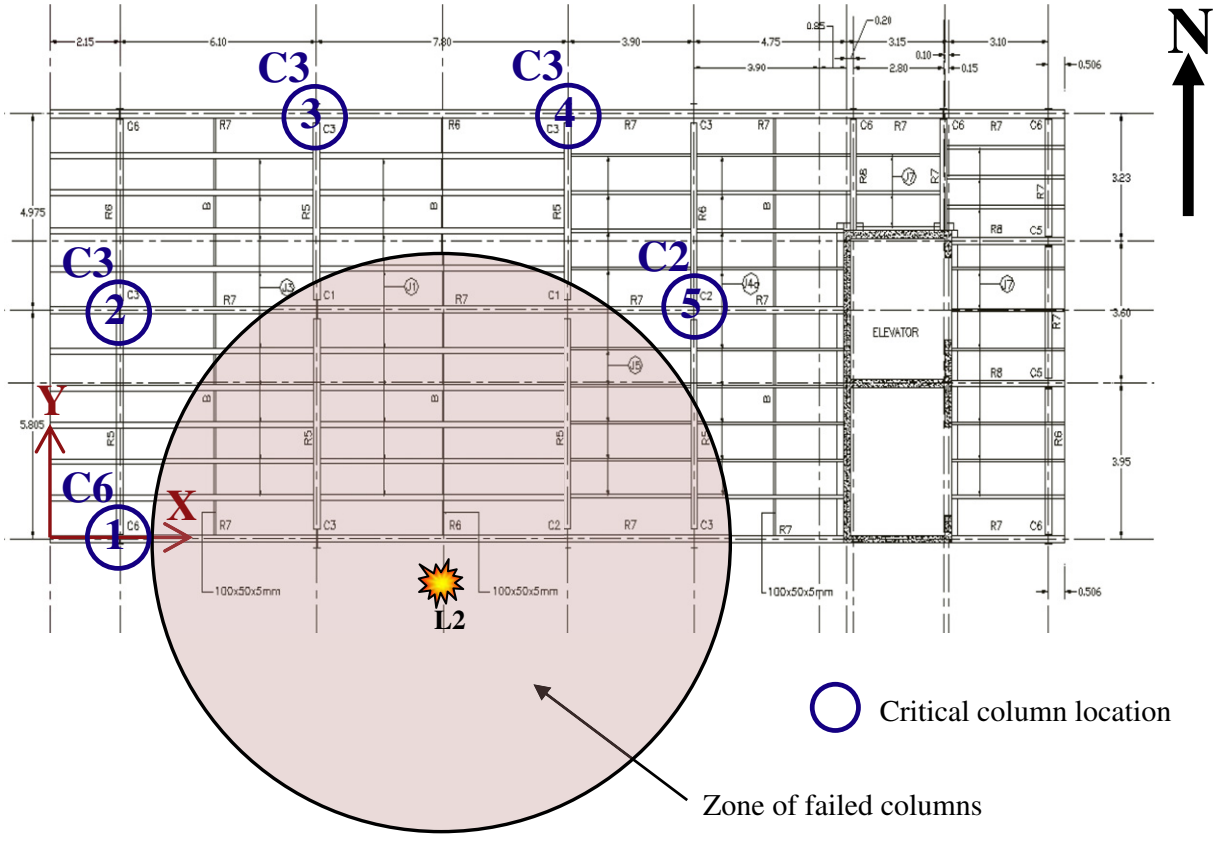

Fig. 14. Zone of failed and critical ground storey columns for blast scenario-2.

of progressive collapse. However, based on the results of the two-stage NLD analysis procedure discussed in the previous sections, the building has a high potential of progressive collapse for the two blast threat scenarios investigated in this study.

The difference between the linear static (LS) analysis procedure of the GSA 2003 Guidelines and the proposed methodology mainly lies in the number of columns removed and the procedure of analysis. The numbers of columns removed in the proposed method are dependent on the blast scenario whereas the GSA Guidelines recommend one-column removal scenario. This discrepancy in the code guidelines and the method of analysis (i.e. LS), which is too simplistic for blast load, are responsible for its non-conservative results for the threat scenarios considered for the building. It is worth mentioning here that most other codes recommend almost similar approach of analysis for the assessment of the progressive collapse potential of buildings. The proposed methodology is thus suggested for the assessment of progressive collapse potential of buildings against blast loads.

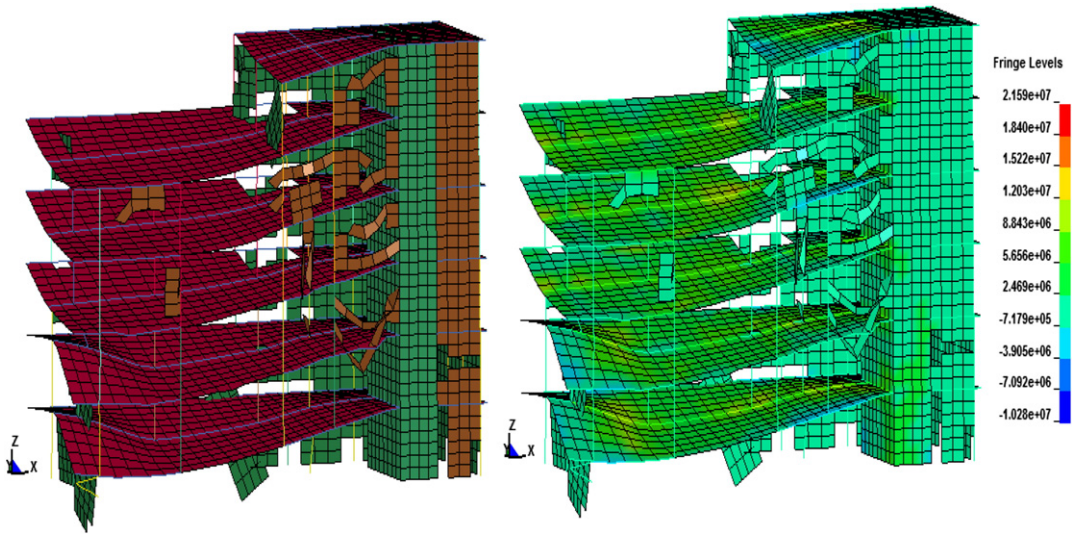

Fig. 15. Partial collapse of building for blast scenario-2.

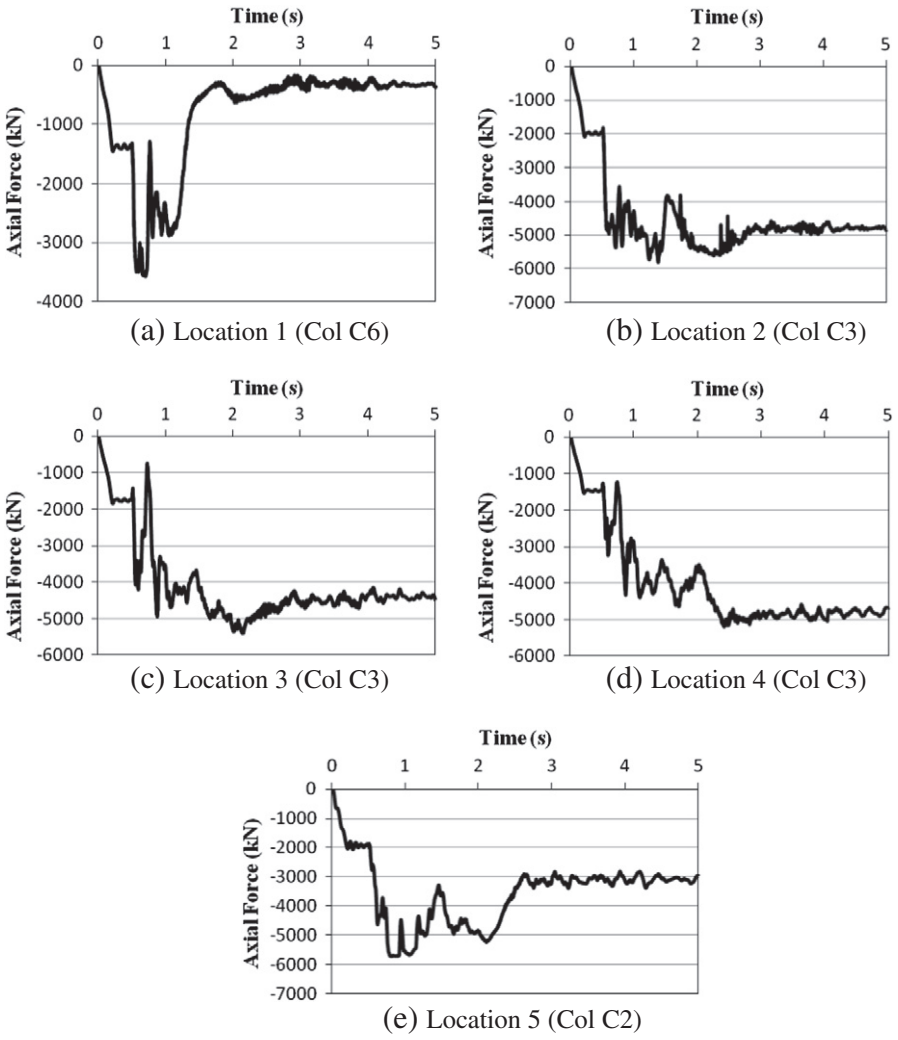

Fig. 16. Variation of axial force with time for critical columns under blast scenario-2.

8. Conclusions

The major conclusions derived from this study are as follows:

1. The 3-D finite element analysis of a typical multi-storey steel framed building located in city of Riyadh shows that the building may undergo progressive collapse even for a charge weight of 500 kg that can be easily carried in a small vehicle. For the two threat scenarios investigated in this study, the charge weight of 500 kg was found enough for causing progressive collapse of the building irrespective of charge location provided it is close to one of the exterior columns.
2. The blast test results of tubular steel beam available in literature were used for the validation of employed numerical models. The deformation response of the beam was compared which showed acceptable prediction.
3. In order to inhibit the progressive collapse potential of the investigated steel building, the stand-off distance of blast must be increased (more than 2 m) by restricting the access of the vehicles to the uilding through perimeter control which may include the

Table 6
Variation of axial load for critical columns of blast scenario-2.

Column location	Column designation	Axial load capacity (P_N) (kN)	Service load (P_s)		Peak load after blast (P_p)		Steady value after blast (P_t)	
			(kN)	P_s/P_N (%)	(kN)	P_p/P_N (%)	(kN)	P_t/P_N (%)
1	C6	3598	1412	39.2	3576	99.4	250	7
2	C3	6500	2000	30.7	5810	89.4	5000	77
3	C3	6500	1729	26.6	5326	82	4500	69.2
4	C3	6500	1439	22.2	5139	79.1	4700	72.3
5	C2	5905	1980	33.5	5720	96.9	2520	42.7

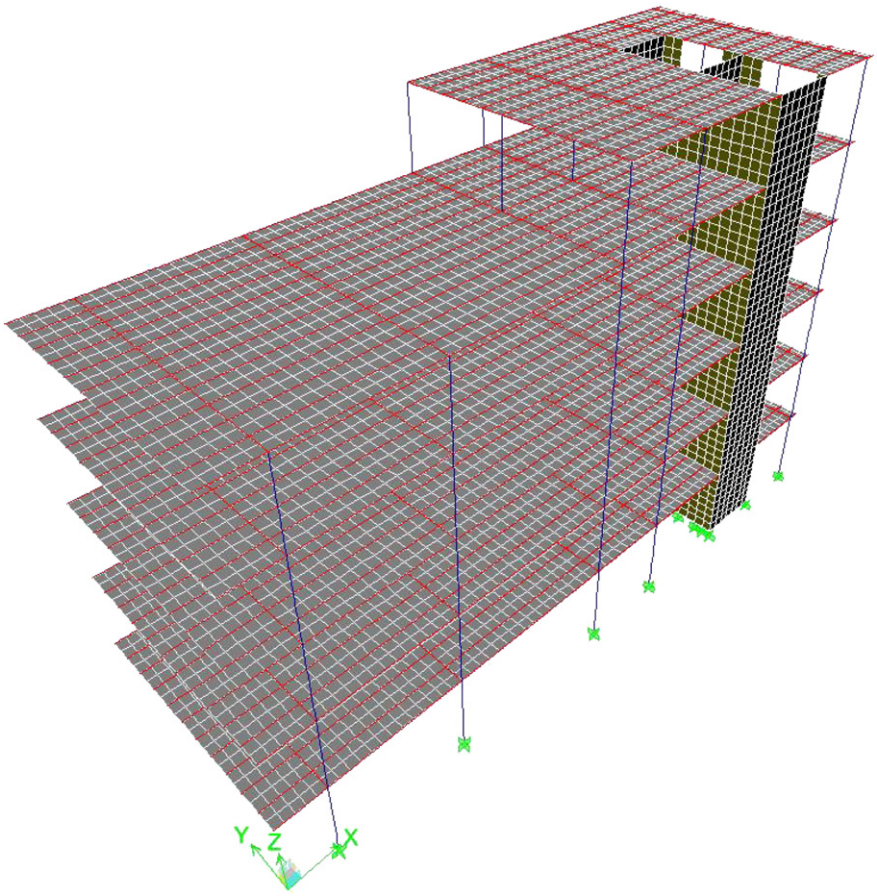

Fig. 17. ETABS 3D model of building.

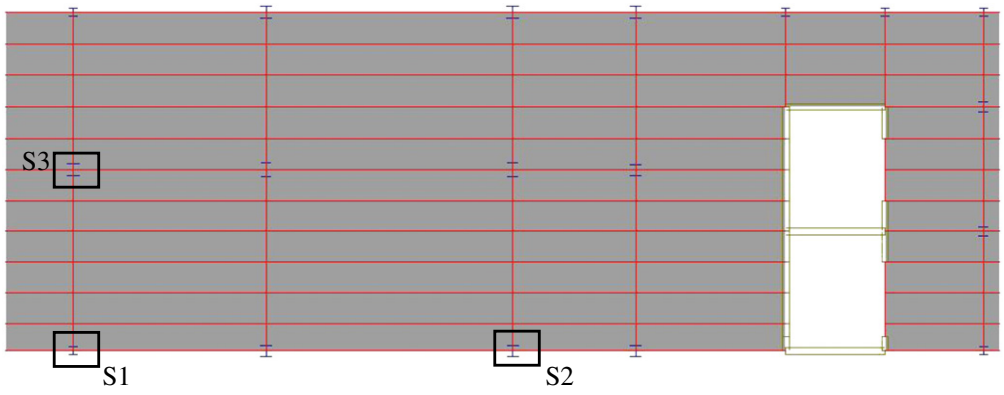

Fig. 18. Missing-column scenarios at ground storey according to the GSA 2003 Guidelines.

introduction of security check points and construction of bollards around the building. If not possible, the outer exposed ground storey columns may need to be strengthened by concrete encasement or addition of steel plates. In case the strengthening of column is not enough for resisting the blast loads due to the possible blast scenarios, some structural modifications should also be considered.

Table 7
DCR values for elements of steel frames (based on results of ETABS models).

GSA 2003 Scenario	Beams		Columns	Potential for progressive collapse
	Flexure	Shear	P-M interaction	
S1	$DCR_{max} = 1.235$ $DCR > 1.0$ for 14 beams	$DCR_{max} = 0.364$	$DCR_{max} = 1.406$ $DCR > 1.0$ for 6 columns	Low
S2	$DCR_{max} = 1.072$ $DCR > 1.0$ for 5 beams	$DCR_{max} = 0.252$	$DCR_{max} = 0.838$	No
S3	$DCR_{max} = 0.99$	$DCR_{max} = 0.527$	$DCR_{max} = 1.671$ $DCR > 1.0$ for 8 columns	Low

The structural modifications may involve the addition of diagonal bracing members or shear walls.

4. The injuries to the occupants of the building due to the flying of the fragments of masonry façade, which is found to fail even in low magnitude of blast, may be minimized through the employment of double-walled façade system.
5. The GSA 2003 Guidelines were followed to assess the progressive collapse potential of the studied steel building using the simplified linear static (LS) analysis procedure. The results were then compared with the two-stage nonlinear dynamic (NLD) analysis procedure developed in this research. It is concluded that in case of blast threat scenarios, the proposed methodology may be more appropriate for the assessment of the progressive collapse potential of steel buildings because the LS analysis of the GSA 2003 Guidelines and other codes may not be conservative for the identified threat scenario.

Acknowledgements

The Authors would like to extend their sincere appreciation to the Deanship of Scientific Research at King Saud University for its funding of this research through the research group project No. RGP-VPP-104.

References

[1] McGuire W. Prevention of progressive collapse. Proc. Regional Conf. on Tall Buildings, Bangkok, Thailand; 1974.
[2] Leyendecker EV, Ellingwood BR. Design methods for reducing the risk of progressive collapse in buildings. Washington, DC: National Bureau of Standards; 1977.
[3] Corley WG, Mlakar PF, Sozen MA, Thornton CH. The Oklahoma City bombing: summary and recommendations for multihazard mitigation. J Perform Constr Facil 1998;12(3):100–12.
[4] Bazant ZP, Zhou Y. Why did the world trade center collapse? Simple analysis. J Eng Mech 2002;128(1):2–6.
[5] Bazant ZP, Verdure M. Mechanics of progressive collapse: learning from world trade center and building demolitions. J Eng Mech 2007;133(3):308–19.
[6] Bazant ZP, Le J, Greening FR, Benson DB. What did and did not cause collapse of world trade center twin towers in New York. J Eng Mech 2008;134(10):892–906.
[7] Seffen KA. Progressive collapse of the world trade center: simple analysis. J Eng Mech 2008;134(2):125–32.
[8] US Department of Defense (DoD). Unified facilities criteria (UFC), DoD minimum antiterrorism standards for buildings. Washington, DC: Department of Defense, UFC 4–010–01, US Army Corps of, Engineering; 2002 31.
[9] General Services Administration (GSA). Progressive collapse analysis and design guidelines for new federal office buildings and major modernization projects. Washington, DC: Office of Chief Architect; 2003.
[10] Marjanishvili S, Agnew E. Comparison of various procedures for progressive collapse analysis. J Perform Constr Facil 2006;20(4):365–74.
[11] Fu F. Progressive collapse analysis of high-rise building with 3-D finite element modeling method. J Constr Steel Res 2009;65:1269–78.
[12] Mohamed OA. Assessment of progressive collapse potential in corner floor panels of reinforced concrete buildings. Eng Struct J 2009;31:749–57.
[13] Khandelwal K, El-Tawil S, Sadek F. Progressive collapse analysis of seismically designed steel braced frames. J Constr Steel Res 2009;65:699–708.
[14] Ruth P, Marchand KA, Williamson EB. Static equivalency in progressive collapse alternate path analysis: reducing conservatism while retaining structural integrity. J Perform Constr Facil 2006;20(4):349–64.
[15] Powel G. Progressive collapse: case studies using nonlinear analysis. Proc. of Metropolis and Beyond-Structures Congress. Reston, VA: ASCE; 2005.
[16] Tsai M, Lin B. Investigation of progressive collapse resistance and inelastic response for an earthquake-resistant RC building subjected to column failure. Eng Struct J 2008;30:3619–28.
[17] Sucuoglu H, Citipitioglu E, Altin S. Resistance mechanisms in RC building frames subjected to column failure. J Struct Eng ASCE 1994;120(3):765–82.
[18] Kim J, Kim T. Assessment of progressive collapse-resisting capacity of steel moment frames. J Constr Steel Res 2009;65:169–79.
[19] Kim J, Dawoon A. Evaluation of progressive collapse of steel moment frames considering catenary action. The structural design of tall and special buildings. 2009;18:455–65.
[20] Grierson D, Safi M, Xu L, Liu Y. Simplified methods for progressive-collapse analysis of buildings. Proc. Metropolis and Beyond, Structures Congress, Reston, VA; 2005.
[21] Izzuddin BA, Vlassis AG, Elghazouli AY, Nethercot DA. Progressive collapse of multi-story buildings due to sudden column loss. Part I: Simplified assessment framework. Eng Struct J 2008;30:1308–18.
[22] Izzuddin BA, Vlassis AG, Elghazouli AY, Nethercot DA. Progressive collapse of multi-story buildings due to sudden column loss. Part II: Application. Eng Struct J 2008;30:1424–38.
[23] Lee C, Kim S, Han K, Lee K. Simplified nonlinear progressive collapse analysis of welded steel moment frames. J Constr Steel Res 2009;65:1130–7.
[24] Naji A, Irani F. Progressive collapse analysis of steel frames: simplified procedure and explicit expression for dynamic increase factor. Int J Steel Struct 2012;12(4):537–49.
[25] Almusallam TH, Elsanadedy HM, Abbas H, Alsayed SH, Al-Salloum YA. Progressive collapse analysis of a RC building subjected to blast loads. Struct Eng Mech 2010;36(3):301–19.
[26] Livermore Software Technology Corporation (LSTC). LS-DYNA user's keyword manual (nonlinear dynamic analysis of structures in three dimensions), vol. 1. Livermore, California: LSTC; 2007 [Version 971].
[27] Elsanadedy HM, Almusallam TH, Abbas H, Al-Salloum YA, Alsayed SH. Effect of blast loading on CFRP-Retrofitted RC columns – a numerical study. Latin Am J Solids Struct 2011;8:5–81.
[28] Kinney GF, Graham KJ. Explosive shocks in air. Berlin: Springer Verlag; 1985.
[29] Conventional weapons effects. Computer software produced by U.S. army Waterways Experimental station, Mississippi, USA; 1990.
[30] Kingery CN, Bulmash G. Airblast parameters from TNT spherical air burst and hemispherical surface burst (No. ARBL-TR-02555). United States Army BRL; 1984.
[31] Smith PD, Hetherington JG. Blast and ballistic loading of structures. Great Britain: Butterworth-Heinemann Ltd; 1994.
[32] Mays GC, Smith PD. Blast effects on buildings: design of buildings to optimize resistance to blast loading. New York, NY: Thomas Telford; 1995.
[33] Belytschko TB, Tsay CS. Explicit algorithms for non-linear dynamics of shells. J Appl Mech ASME 1981;48:209–31.
[34] Jama HH, Bambach MR, Nurick GN, Grzebieta RH, Zhao X. Numerical modelling of square tubular steel beams subjected to transverse blast loads. Thin-Walled Struct 2009;47:1523–34.
[35] Shi Y, Hao H, Li Z. Numerical derivation of pressure-impulse diagrams for prediction of RC column damage to blast loads. Int J Impact Eng 2008;35:1213–27.
[36] ANSI/AISC 360-05. Specifications for structural steel buildings. American Institute of Steel Construction, Chicago, IL, USA; 2005.
[37] Computers and Structures, Inc. ETABS nonlinear version 9.7.4 – extended 3D analysis of building systems. Berkeley, CA, USA: CSI; 2011.
[38] Marchis A, Botez M, Ioani AM. Vulnerability to progressive collapse of seismically designed reinforced concrete framed structures in Romania. Proc of the 15th World Conf on Earthquake Eng. (WCEE), Lisbon, Portugal; 2012.